Cubic-Grid Gaussian Basis Sets for Electron-Scattering Calculations. 6. Applications to H_2, H_2O, and CH_4

Petr Čársky* and Vojtěch Hrouda

J. Heyrovský Institute of Physical Chemistry, Academy of Sciences of the Czech Republic, Dolejškova 3, 18223 Prague 8, Czech Republic

Martin Polášek

Faculty of Science and Philosophy, Silesian University, Bezručovo nám. 13, 74601 Opava, Czech Republic

Donald E. David, Dean Antic, and Josef Michl

Department of Chemistry and Biochemistry, University of Colorado at Boulder, Boulder, Colorado 80309-0215

Received: July 1, 1996; In Final Form: December 30, 1996[⊗]

We present a vibrational electron energy loss spectrum (EELS) of neat solid methane, with partially resolved bands for ν_4 and ν_2 excitations. The intensities of the observed bands are well reproduced by scattering calculations performed by the recently developed cubic-grid Gaussian basis set (CGGBS) method. For testing the CGGBS method we also used literature data on elastic electron scattering by methane and data on elastic and vibrational inelastic electron scattering by H_2 and H_2O. We present a procedure for the analytical differentiation of the scattering amplitude with respect to normal coordinates.

Introduction

Our interest in the theory of electron scattering arose from a need to interpret and better understand electron energy loss spectra (EELS) measured at the University of Colorado at Boulder. So far, EELS and electron scattering in general have been mostly a domain of physicists. In chemistry, EELS has been used almost exclusively as an analytical tool for identification of species adsorbed on a metal surface, without much detailed understanding of the scattering process. Notable exceptions have been the work of Allan,[1,2] Kuppermann,[3] Jordan and Burrow,[4] McKoy[5,6] and their collaborators, and some other chemically oriented papers on gas-phase electron−molecule scattering. We believe that this kind of spectroscopy could be more frequently exploited in chemistry for observation of transitions that are forbidden in photon spectroscopy and for a better understanding of the electronic structure of chemisorbed species. Recently, we constructed at Boulder an instrument for the measurement of EELS of matrix-isolated molecules at 5 K. This extends the applicability of EELS to matrix-isolated reaction intermediates and other unstable species of unusual structures. As with other kinds of spectroscopy, unusual electronic structure of such species may give rise to unusual features in EELS. Moreover, the use of matrix isolation brings new problems and opportunities to EELS that are absent in gas-phase experiments. They are a direct effect of the noble gas atoms on the electronic structure of matrix-isolated molecules, possible diffraction of electrons in the matrix, possible alignment of molecules in the matrix, and reflection of electrons from a silver surface on which the argon matrix is deposited. Firm interpretation of the measured spectra therefore requires a theoretical tool that would provide a reliable prediction of relative intensities in vibrational and electronic EELS of molecules. In the last two years we have developed[7−11] a computational method that should meet this need, based on *ab initio* treatment of the Lippmann−Schwinger equation. For this purpose we have developed[7] cubic-grid Gaussian basis sets (CGGBSs) consisting of s-type Gaussians centered at the points of a regular lattice. They were constructed with the aim of obtaining the best fit for the plane-wave function $|k\rangle = \exp(ikr)$. The CGGBSs subject to this condition give correct first Born terms. The same Gaussian expansion of $|k\rangle$ was also used in the expression for the Green's function operator, and integration over the k vector then resulted in a separable form of the Green's function operator.[8] In this way we bypassed the insertion of an approximate separable potential used in the **T**-matrix expansion method[12] to express the *UGT* term in the Lippmann−Schwinger equation as a product of three matrix elements over Gaussian functions. In order to reduce the number of CGGBS functions, only those Gaussians are retained that lie inside a sphere with a preselected diameter. The parameters determining the basis set, namely, a common Gaussian exponent and lattice constant, depend only on the energy of the incident electron. The use of two different basis sets—CGGBS for plane-wave functions and molecular Gaussian basis set for the interaction potential—does not guarantee translational and rotational invariance of the calculated differential cross section with respect to position of the target molecule in the sphere limiting the space for CGGBS. However, test calculations[9] showed a near invariance of the calculated differential cross section for small shifts of the molecule, provided that the molecule remained located near the center of the sphere. Next, we derived formulas for accounting for the long-range part of the interaction between the scattering electron and the target molecule[9] and formulas for analytical averaging of the differential cross section over all possible orientations of the target molecule[10] and improved the static-exchange approach by adding to the interaction potential the second-order correction[13] for polarization effects.

Computational methods of this type have already been developed (see, for example, refs 14 and 15), but they were mostly tailored for gas-phase electron elastic scattering by diatomic molecules. In 1986 Gianturco and Jain stated[15] that "the whole area of large molecules is still in its infancy as far as theoretical treatments go", and the situation has not changed

[⊗] Abstract published in *Advance ACS Abstracts,* May 1, 1997.

S1089-5639(96)01934-2 CCC: $14.00

dramatically since that time, though a few papers on polyatomic molecules were published such as those by McKoy and collaborators on ethylene,[16] propene,[17] cyclopropane,[17] and [1.1.1]propellane.[18]

We first tested the CGGBS method for three simple empirical potentials:[11] exponential ($V = \exp(-ar)$), Gaussian ($V = \exp(-ar^2)$), and Yukawa ($V = \exp(-ar)/r$). We calculated the angular dependence of the differential cross section by solving the Lippmann−Schwinger equation. The results obtained for the CGGBS were in quantitative agreement with the data obtained by a direct numerical solution of the Lippmann−Schwinger equation. Next, we decided to undertake a systematic study of small molecules. We performed a literature search on elastic and vibrational inelastic electron scattering by small molecules and selected papers dealing with the molecules H_2, H_2O, and CH_4 for incident electron energy of 6−20 eV. For CH_4 we also present our own EELS spectrum.

Theoretical Section

Calculations on elastic electron scattering were performed as described in our previous papers.[7−10] For the target molecules H_2, H_2O, and CH_4 we used Sadlej's [5s3p1d/3s1p] basis sets,[19] which were especially developed for SCF calculations of electric properties and should therefore be suitable for SCF calculations of the potential between the target molecule and a scattering electron. The molecular geometries were optimized by SCF calculations, and the optimum geometries and the molecular orbitals obtained at optimum geometries were then used in scattering calculations.

In vibrationally inelastic scattering calculations we considered it natural to try the procedure that has been used routinely and successfully in applications of the molecular structure theory to problems of infrared spectroscopy. The essence of this procedure is the adoption of the harmonic approximation. Hence, starting from the general expression for the differential cross section

$$\left(\frac{d\sigma}{d\Omega}\right)_k = \langle \chi_{1,k}\, k_{out}|T|k_{in}\chi_{0,k}\rangle \tag{1}$$

the **T**-matrix element for the vibrational excitation $0 \leftarrow 1$ may be approximated as[8]

$$\langle \chi_{1,k}\, k_{out}|T|k_{in}\chi_{0,k}\rangle = 2^{-1/2}\left(\frac{\partial T_{out,in}}{\partial q_k}\right)_0 \tag{2}$$

in analogy with the standard treatment of the dipole moment operator. In eqs 1 and 2 the plane-wave functions are assumed to be unnormalized, $\chi_{1,k}$ and $\chi_{0,k}$ are the respective vibrational functions, q_k is the dimensionless kth normal coordinate, and $T_{out,in}$, which depends only on electronic coordinates, is given by

$$T_{out,in} = \langle k_{out}|T|k_{in}\rangle \tag{3}$$

Since in the CGGBS expansion[7,8] the expansion coefficients do not depend on normal coordinates, the derivative of $T_{out,in}$ at the equilibrium geometry with respect to the normal coordinate q_k may be expressed as

$$\left(\frac{\partial T_{out,in}}{\partial q_k}\right)_0 = F_{in}\, F_{out} \sum_{ij} \langle k_{out}|s_i\rangle \left(\frac{\partial T_{ij}}{\partial q_k}\right)_0 \langle s_j|k_{in}\rangle \tag{4}$$

Differentiation in eq 2 may be done numerically or analytically. In the two-sided numerical differentiation we used the step size $q_k = 0.5$. Averaging of the calculated cross section over the isotropic orientation of the target molecule with respect to the directions of the incoming and scattering electron was performed in the same way as in the case of elastic scattering.[10]

In the analytical calculation of vibrationally inelastic scattering cross sections, the expression for the derivative $\partial T/\partial q$ is obtained from the differentiation of the Lippmann−Schwinger equation. Since the **G** matrix in the CGGBS basis set does not depend on the atomic coordinates of the target molecule, the first derivative of the Lippmann−Schwinger equation for each coordinate becomes

$$\mathbf{T}^{(1)} = \mathbf{U}^{(1)} + \mathbf{U}^{(1)}\mathbf{G}_0\mathbf{T} + \mathbf{U}\mathbf{G}_0\mathbf{T}^{(1)} \tag{5}$$

As in quantum chemical calculations,[20] we evaluate first the derivatives in Cartesian coordinates. For each coordinate x we construct first derivative matrix $\mathbf{T}^{(1)}$ with the elements in the CGGBS

$$T_{ij}^{(1)} = \frac{\partial T_{ij}}{\partial x} \tag{6}$$

By matrix inversion we obtain

$$\mathbf{T}^{(1)} = (1 - \mathbf{U}\mathbf{G}_0)^{-1}\mathbf{U}^{(1)}\,(1 + \mathbf{G}_0\mathbf{T}) \tag{7}$$

In the static-exchange approximation the $\mathbf{U}^{(1)}$ matrix elements for a closed shell molecule are given as

$$\mathbf{U}^{(1)} = 2\mathbf{V}^{(1)} \tag{8}$$

$$\frac{\partial V_{\alpha\beta}}{\partial x} = \left\langle \alpha \left| \frac{\partial}{\partial x} \sum_A \frac{Z_A}{|r - R_A|} \right| \beta \right\rangle + 2\sum_{\mu\nu} P_{\mu\nu} \frac{\partial}{\partial x}\langle \mu\alpha|\nu\beta\rangle - \sum_{\mu\nu} P_{\mu\nu} \frac{\partial}{\partial x}\langle \mu\nu|\alpha\beta\rangle + 2\sum_{\mu\nu}\left(\frac{\partial P_{\mu\nu}}{\partial x}\right)\langle \mu\alpha|\nu\beta\rangle - \sum_{\mu\nu}\left(\frac{\partial P_{\mu\nu}}{\partial x}\right)\langle \mu\nu|\alpha\beta\rangle \tag{9}$$

The symbol x stands for a nuclear displacement, and the other symbols have their usual meaning; Z_A and R_A are nuclear charges and position vectors of nuclei in the target molecule, $P_{\mu\nu}$ is the density matrix and in the two-electron integrals defined as

$$\langle pq|rs\rangle = \int\int \chi_p(1)\chi_q(2)\,\frac{1}{r_{12}}\,\chi_r(1)\chi_s(2)\,d\tau_1\,d\tau_2 \tag{10}$$

the μ and ν indices refer to the Gaussian basis set functions of the target molecule and α and β to the CGGBS functions. Our derivation is intentionally similar to the derivation of the Hessian in the Hartree−Fock theory.[20] This permits us to use routines for a coupled perturbed Hartree−Fock procedure that are available in common codes for *ab initio* MO calculations and that are also required for the analytical gradient of the scattering amplitude.

If the polarization effect is included by means of the second-order correction,[13] eq 7 may be still used, but the expression for $\partial V_{\alpha\beta}/\partial x$ would be more complicated and similar to the expression[20] for the derivative of the second-order correlation energy MP2. We did not attempt to program this, and when the polarization effect was included, we differentiated the **T**-matrix element in eq 1 numerically. However, we had to use a smaller grid ($q = 0.1$) because the dependence of ΔT on Δq was less linear than in the absence of polarization. In either case, the averaging of the differential cross section with respect to the target molecule orientation was performed in the same way as in calculations on elastic scattering.[10]

TABLE 1: Averaged Differential Cross Sections for the a_1 Stretching Mode of Methane

	$d\sigma/d\Omega$ (10^{-18} cm^2/sr)	
scattering angle θ (deg)	analytical[a]	numerical[b]
0	0.911	0.910
20	0.526	0.524
40	0.116	0.115
60	0.161	0.160
80	0.256	0.256
100	0.254	0.253
120	0.190	0.189
140	0.173	0.173
160	0.287	0.285
180	0.373	0.371

[a] Analytical differentiation of the scattering amplitude. [b] Calculated by numerical differentiation of the scattering amplitude.

Most calculations of vibrational differential cross sections without the polarization correction were run in parallel by using analytical and numerical differentiation of the scattering amplitude. In all cases the agreement was very satisfactory. As an example, we present in Table 1 the results for the a_1 stretching mode of methane, which were obtained with the $9 \times 9 \times 9$ CGGBS basis set for the electron impact energy of 20 eV.[7] In both numerical and analytical calculations we obtained the same intensities for components of degenerate modes of CH_4; the discrepancies represented a few percent of the absolute value of the calculated differential cross section. This served as another test of the computer code.

Experimental Section

The EELS spectrum of neat methane (Matheson, UHP grade, used as received) was measured with an LK 2000 spectrometer modified for position-sensitive detection. Details of the modification will be described in a later publication. The sample (50 Å) was deposited on a Ag(111) substrate and measured at 5 K. The primary electron beam (20 eV) had an incidence angle of 45° on the substrate. The scattered electrons were measured at a fixed angle of 60° relative to the forward direction, i.e., 30° off the specular direction, precluding any contribution by specular reflection from the substrate or sample.

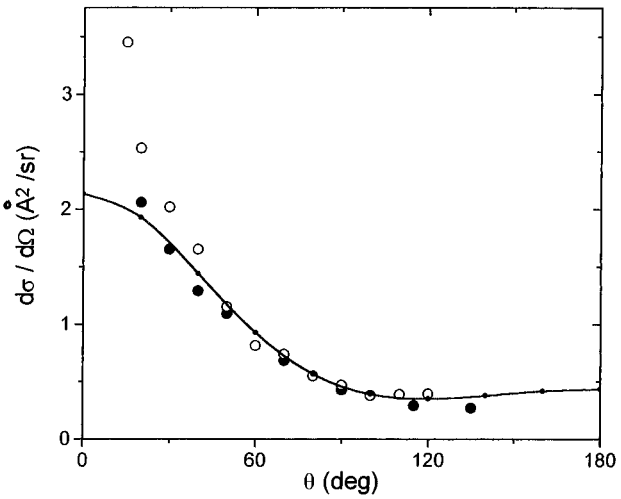

Figure 1. Differential cross section for elastic electron scattering by H_2 at 10 eV calculated with the half-spaced $13 \times 13 \times 13$ CGGBS, with the [7s5p] basis set for H_2, and with the second-order polarization term included. Full circles denote experimental data by Srivastava et al.[21] renormalized by Trajmar et al.[22] Open circles denote experimental data of Nishimura et al.[23]

Results and Discussion

Elastic Scattering. The H_2 molecule is among those that have been studied experimentally most extensively. We looked for data on elastic electron scattering by H_2 at the electron energy of 10 eV because we anticipate that it will be a typical value for our future vibrational EELS experiments. Figure 1 shows the experimental data originating from two different laboratories[21−23] together with the results of our most extensive

TABLE 2: Differential Cross Sections for Elastic Electron Scattering by H_2[a] Calculated with CGG Basis Sets

	$d\sigma/d\Omega$ (au)				
scattering angle θ (deg)	$7 \times 7 \times 7$	$9 \times 9 \times 9$	$11 \times 11 \times 11$	$13 \times 13 \times 13$	$15 \times 15 \times 15$
0	6.881	6.382	6.273	6.294	6.309
20	6.254	5.783	5.692	5.720	5.725
40	4.744	4.378	4.324	4.342	4.339
60	3.117	2.905	2.869	2.872	2.880
80	1.938	1.863	1.848	1.855	1.852
100	1.349	1.356	1.365	1.363	1.358
120	1.209	1.239	1.262	1.252	1.252
140	1.296	1.309	1.342	1.331	1.328
160	1.424	1.410	1.452	1.440	1.432
180	1.480	1.453	1.498	1.487	1.475

[a] Sadlej's basis set was used for the H_2 molecule, and the polarization term was included. Electron impact energy: 10 eV.

TABLE 3: Differential Cross Sections for Elastic Electron Scattering by H_2 Calculated with the $11 \times 11 \times 11$ CGGBS[a]

	$d\sigma/d\Omega$ (au)			
scattering angle θ (deg)	[3s1p] no polarization	[3s1p] polarization	[7s5p] no polarization	[7s5p] polarization
0	4.886	6.273	5.097	6.582
20	4.478	5.691	4.668	5.954
40	3.514	4.324	3.646	4.481
60	2.468	2.869	2.537	2.933
80	1.717	1.848	1.743	1.869
100	1.350	1.365	1.357	1.378
120	1.268	1.262	1.270	1.275
140	1.333	1.342	1.333	1.352
160	1.425	1.452	1.425	1.456
180	1.465	1.498	1.464	1.500

[a] Electron impact energy: 10 eV.

TABLE 4: Differential Cross Sections for Elastic Electron Scattering by H_2 Calculated with the Half-Spaced 13 × 13 × 13 CGGBS[a]

	dσ/dΩ (au)			
scattering angle θ (deg)	[3s1p] no polarization	[3s1p] polarization	[7s5p] no polarization	[7s5p] polarization
0	5.682	6.984	5.857	7.325
20	5.207	6.358	5.356	6.632
40	4.064	4.857	4.155	4.988
60	2.817	3.230	2.852	3.252
80	1.881	2.036	1.885	2.018
100	1.388	1.421	1.382	1.412
120	1.261	1.273	1.255	1.274
140	1.340	1.378	1.334	1.373
160	1.463	1.532	1.457	1.515
180	1.518	1.600	1.511	1.576

[a] Electron energy: 10 eV.

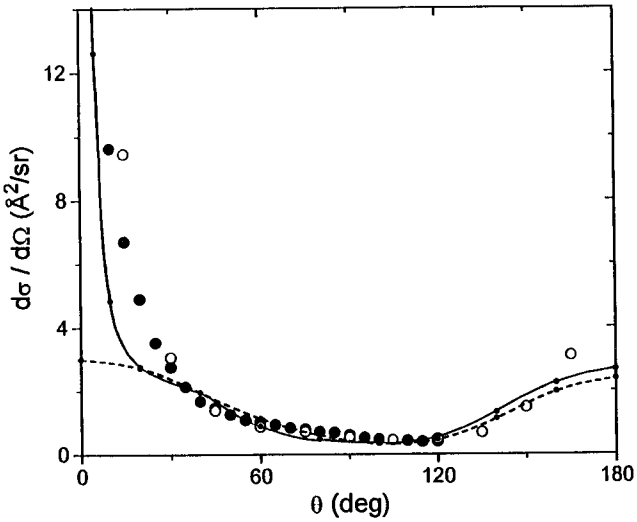

Figure 2. Differential cross section for elastic electron scattering by H_2O at 10 eV calculated with the half-spaced 13 × 13 × 13 CGGBS, with Sadlej's [5s3p1d/3s1p] basis set for the H_2O molecule, with second-order polarization, and with the long-range term (solid line). The dashed line results when the long-range term is omitted. Experimental data are taken from papers by Shyn et al.[26] (○) and by Johnstone and Newell[27] (●).

calculation. The results of our other calculations on the elastic electron scattering by H_2 are presented in Tables 2−4. These were obtained with and without the second-order polarization correction,[10,13] with regular and half-spaced CGGBS basis sets for the scattering electron, and with Sadlej's[19] [3s1p] and large Huzinaga's[24] (10s5p)/[7s5p] basis sets for the H_2 molecule. In all these calculations the interatomic distance $R_{HH} = 1.4$ au was assumed. Table 2 shows the effect of extending the Gaussian representation of plane-wave functions, on going from the 7 × 7 × 7 CGGBS basis set with 123 Gaussians to the 15 × 15 × 15 basis set with 1419 Gaussians. The convergence is good, and it is seen that only very little can be gained upon further extension of the CGGBS basis set. The effect of the CGG basis set choice on the calculated cross section has been investigated elsewhere[9] for He and Ne atoms and for the H_2O molecule. The conclusion was that 11 × 11 × 11 was the best compromise between complete elastic DCS convergence and cost of computation. Tables 3 and 4 indicate that Sadlej's basis set is sufficiently large and that further extension of the basis set for the target molecule brings only a minor improvement in the calculated differential cross section. We also found the same effect in tests on other target molecules, and we decided therefore to use Sadlej's basis sets as standard basis sets. In accordance with what is known in the literature,[25] Tables 3 and 4 show that the polarization effect is very important, particularly at small scattering angles. Table 4 presents the results obtained

TABLE 5: Differential Cross Sections for Elastic Electron Scattering by CH_4 Calculated[a] with Three Different CGGBS without (noP) and with (P) Second-Order Polarization

	dσ/dΩ (Å²/sr)					
	7 × 7 × 7		11 × 11 × 11		half-spaced 13 × 13 × 13	
scattering angle θ (deg)	noP	P	noP	P	noP	P
0	5.170	8.624	5.658	7.849	4.878	7.795
20	4.201	6.572	4.645	5.991	3.741	5.738
40	2.387	2.886	2.800	2.915	1.727	2.210
60	1.295	1.105	1.625	1.549	0.718	0.719
80	0.973	1.201	1.055	1.292	0.615	0.908
100	0.753	1.250	0.636	0.909	0.617	0.976
120	0.657	0.907	0.519	0.633	0.851	0.946
140	1.100	1.173	0.939	0.998	1.789	1.795
160	1.904	2.164	1.611	1.743	3.083	3.307
180	2.315	2.740	1.936	2.119	3.702	4.082

[a] Electron impact energy: 10 eV.

with the half-spaced basis set. In this approach the diameter of the sphere limiting the space for the CGGBS representation of the plane wave is half of that of the corresponding "regular" CGGBS sphere. In order to keep the diameter of the sphere sufficient, we used the 13 × 13 × 13 CGGBS, which has 13 Gaussians on the diameter and a total of 925 Gaussians inside the sphere. Being more densely packed, the half-spaced CGGBS gives a more accurate Green's function.[7] The effect on the calculated differential cross section is seen from the comparison of entries in Tables 3 and 4. Next, doubling of the linear density by going to a quarter-spaced grid would increase the number of basis set functions by a factor of 8. This would make the calculations extremely difficult to perform, and the enormous increase of the cost would not be worth the few percent gained in convergence with respect to the exact results. In our previous paper[9] we also examined the variation in the scattering cross section as a function of position of the target molecule with respect to the fixed grid of Gaussians. For the larger basis sets we found that both elastic and inelastic cross sections for the water molecule were almost invariant with regard to displacement of the molecule in the Gaussian grid.

Calculation of elastic electron scattering by H_2O at 10 eV turned out to be more difficult. For scattering angles from 80 to 180° the agreement with experimental results was good, and the calculated differential cross section depended very little on the size of the CGGBS basis set. Also, the effect of polarization was marginal. For lower scattering angles, 30−60°, good agreement with experimental results was achieved only with the half-spaced 13 × 13 × 13 CGGBS basis set, and, as seen in Figure 2, the range of even lower scattering angles was reproduced only when the long-range term[9] was included.

Results of our CGGBS calculations on elastic electron scattering by CH_4 at 10 and 20 eV are summarized in Tables 5

TABLE 6: Differential Cross Sections for Elastic Electron Scattering by CH_4 Calculated[a] with Three Different CGGBS without (noP) and with (P) Second-Order Polarization

	dσ/dΩ (Å²/sr)					
	7 × 7 × 7		11 × 11 × 11		half-spaced 13 × 13 × 13	
scattering angle θ (deg)	noP	P	noP	P	noP	P
0	9.014	10.917	9.555	12.432	8.765	10.262
20	6.711	8.077	6.741	8.470	6.366	7.325
40	2.541	2.976	2.445	2.775	2.315	2.529
60	0.454	0.455	0.782	0.913	0.533	0.602
80	0.612	0.661	0.696	0.865	0.629	0.770
100	0.984	1.114	0.645	0.729	0.820	0.924
120	0.706	0.749	0.423	0.435	0.637	0.658
140	0.336	0.279	0.264	0.228	0.440	0.410
160	0.323	0.314	0.234	0.172	0.439	0.416
180	0.407	0.464	0.243	0.175	0.484	0.478

[a] Electron energy: 20 eV.

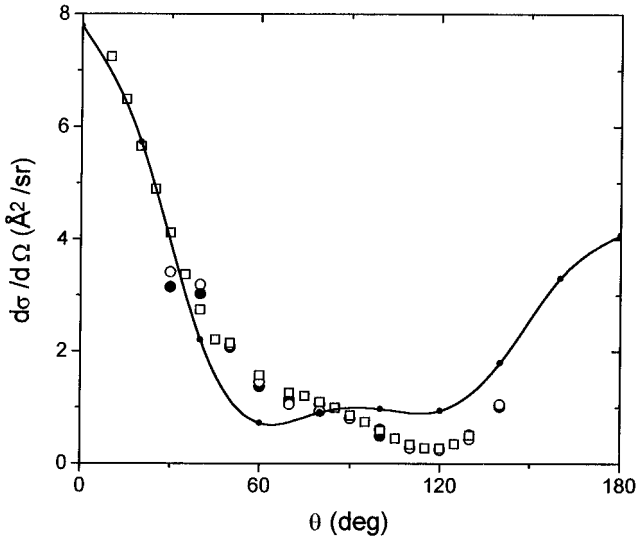

Figure 3. Differential cross section for elastic electron scattering by CH_4 at 10 eV calculated with the half-spaced 13 × 13 × 13 CGGBS, with Sadlej's [5s3p1d/3s1p] basis set for CH_4, and with second-order polarization included. Circles are experimental data by Curry et al.[28] (○) and by Tanaka et al.[29] (●), and squares (□) are experimental data by Boesten and Tanaka.[30]

and 6. The entries in these tables show the effect of polarization, the effect of the size of CGGBS, and the effect of using a more densely packed CGGBS, the half-spaced CGGBS. It is seen that all three effects are noticable in this case, though they are not dramatic. Calculations with the single-spaced or double-spaced 13 × 13 × 13 CGGBS and with the second-order polarization term included most likely provide results close to the convergence limit of the CGGBS approach. Such calculations are now feasible on workstations for molecules of moderate size. The calculations with the half-spaced 13 × 13 × 13 basis set represent our most extensive calculations on CH_4, and they are plotted in Figures 3 and 4 along with the experimental data obtained by Curry et al.,[28] Tanaka et al.,[29] and Boesten and Tanaka.[30] Our calculations reproduce satisfactorilly the observed angular dependence, though they do not match the experimental data as closely as the more sophisticated multichannel scattering calculations by Lima et al.[31]

We have focused our attention on the angular dependence of the differential cross section at a few selected energies. This was dictated in part by the nature of the experimental data we are collecting. In a matrix, we cannot use electron energies higher than about 20 eV, and the theoretical method based on a single-channel static-exchange approach with a second-order

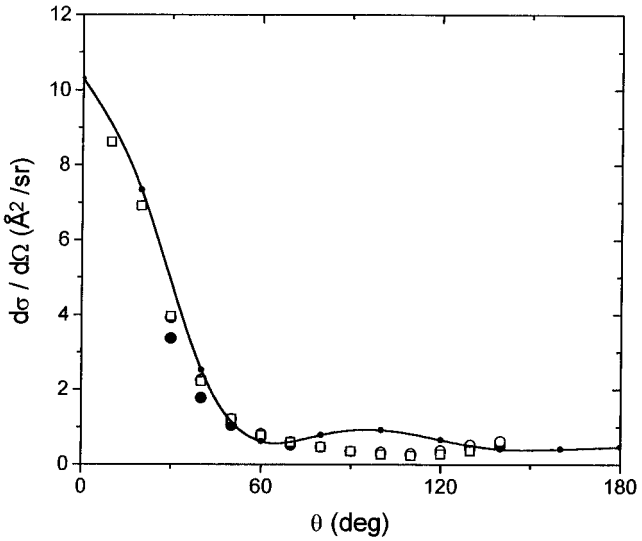

Figure 4. Differential cross section for elastic electron scattering by CH_4 at 20 eV calculated with the half-spaced 13 × 13 × 13 CGGBS, with Sadlej's [5s3p1d/3s1p] basis set for CH_4, and with second-order polarization included. Circles are experimental data by Curry et al.[28] (○) and by Tanaka et al.[29](●), and squares (□) are experimental data by Boesten and Tanaka.[30]

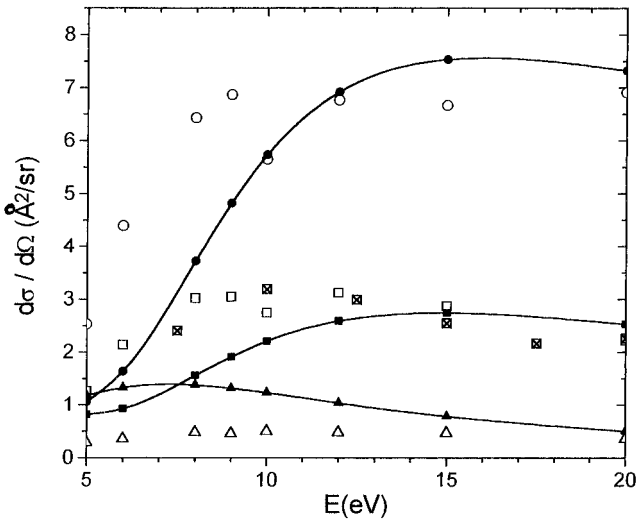

Figure 5. Energy dependence of the differential cross section for elastic electron scattering by CH_4 at three scattering angles: 20° (circles), 40° (squares and squares with crosses), and 130° (triangles). Lines and full marks represent data calculated with the half-spaced 13 × 13 × 13 CGGBS, with Sadlej's basis set for CH_4, and with the second-order polarization term included. Open marks are experimental data by Boesten and Tanaka,[30] and by Curry et al.[28] (squares with crosses).

correction for polarization effects cannot be expected to work below about 5 eV. Still, we wanted to check whether the theory can reproduce the energy dependence of the differential cross section of the electron elastic scattering by methane in this limited energy range. We selected three scattering angles and plotted the calculated cross sections in Figure 5 as a function of electron energy. It is seen that the calculated energy dependence reproduces qualitatively the observed data, though the agreement becomes worse at lower energies, as expected. Unlike the scattering cross sections measured by Boesten and Tanaka,[30] our calculations, and the experimental data reported by Curry et al.,[28] do not indicate any minimum at 10 eV.

Vibrational Inelastic Scattering. For H_2 we calculated the vibrational cross sections by means of two-sided numerical differentiation, assuming $R_{HH} = 1.40$ au for the reference geometry and $q = \pm 0.5$ for the distorted structures. The results

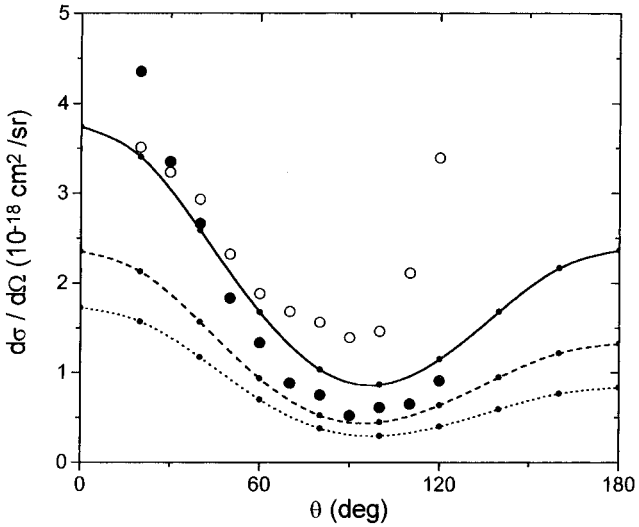

Figure 6. Differential cross section for vibrational excitation in H_2 at 6 eV calculated with Sadlej's [3s1p] basis set for H_2 and the 11 × 11 × 11 CGGBS without (dotted line) and with (dashed line) the second-order polarization, and the half-spaced 13 × 13 × 13 CGGBS with polarization (full line). Experimental data are taken from papers by Nishimura et al.[23] (○) and by Linder and Schmidt[32] (●).

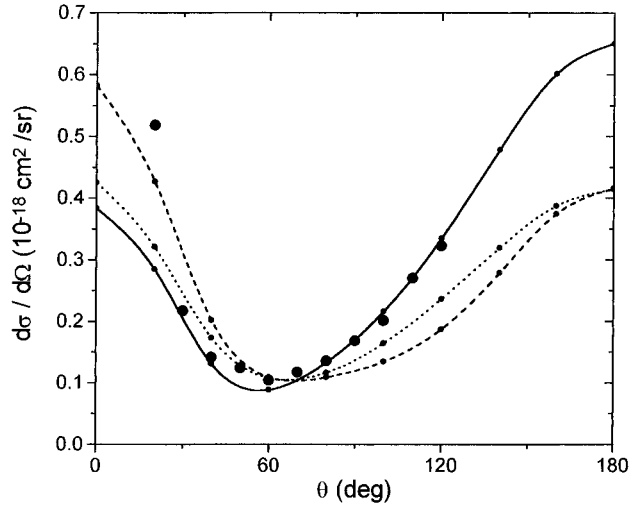

Figure 7. Differential cross section for vibrational excitation in H_2 at 20 eV calculated as specified in Figure 5. Full circles are experimental data by Nishimura et al.[23]

calculated for electron energies of 6 and 20 eV are presented in Figures 6 and 7, where they are plotted together with the experimental data by Nishimura et al.[23] and Linder and Schmidt.[32] Although the H_2 molecule belongs to molecules studied experimentally most extensively,[22] the data originating from different laboratories differ considerably. As Figure 7 shows, our results obtained with the most extensive calculation for the electron impact energy of 6 eV lie in between, except for the region of lowest scattering angles for which it generally seems to be difficult for reproducing the experimental results. Perfect agreement of the calculations obtained for 20 eV with the data by Nishimura et al.[23] is most likely fortuitous. On the other hand, at 20° the agreement between theory and experiment may be better than Figure 7 suggests. The two figures agree with the known fact that the effect of polarization is more important at lower energies. Figure 6 also shows that at 6 eV the calculated differential cross section depends strongly on the size of CGGBS.

The cross section of the vibrational excitation of H_2O stretching modes, plotted against electron energy, shows a

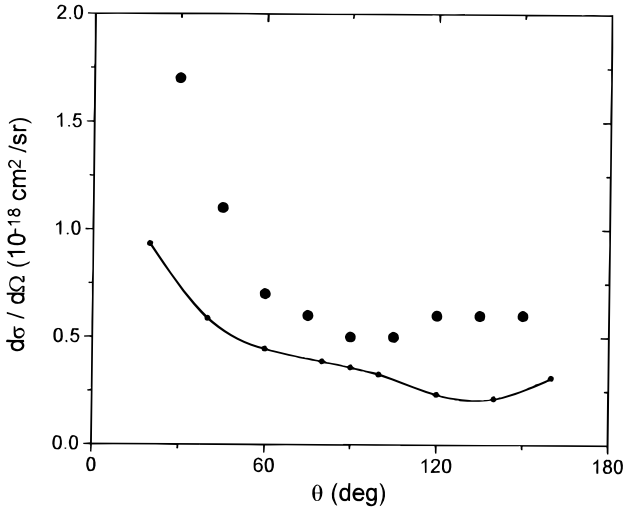

Figure 8. Angular dependence of the differential cross section at 20 eV for the bending mode of the water molecule calculated with the half-spaced 13 × 13 × 13 CGGBS. Full dots are experimental data taken from ref 33.

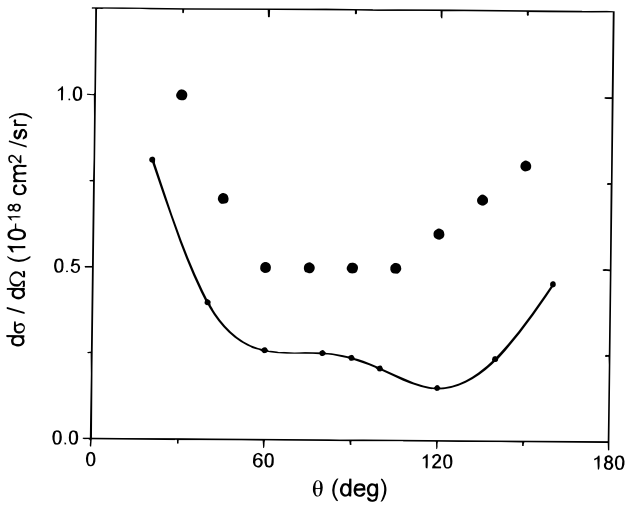

Figure 9. Angular dependence of the differential cross section at 20 eV for a joint excitation of the two stretching modes of the water molecule calculated with the half-spaced 13 × 13 × 13 CGGBS basis set. Full dots are experimental data taken from ref 33.

distinct resonance band[33,34] with a maximum at 6−8 eV. Since up to now our computer program cannot take into account the effect of bound states of H_2O-e^-, we decided to perform calculations only outside the range of resonances. In Figures 8 and 9 we present the results of our calculations at 20 eV. The stretching modes are plotted together in Figure 9 because the resolution of observed EELS spectra is not sufficient to resolve the two modes.[33,34] The polarization effect is not included in these calculations. The differentiation of the scattering amplitude could only be performed numerically in this case, and we found that the derivative depended greatly on the step size. We decided therefore to limit ourselves to calculations without polarization that were free of this numerical problem and for which the results of analytical and numerical differentiation with different step sizes were in a very good agreement. Neglect of polarization is a probable reason for the calculated differential cross sections being too low. As noted below, for methane we found that probabilities of vibrational excitations are increased upon inclusion of the polarization effect. If this trend also applies to the H_2O molecule, the calculated data corrected for polarization would match better the experimental data plotted in Figures 8 and 9.

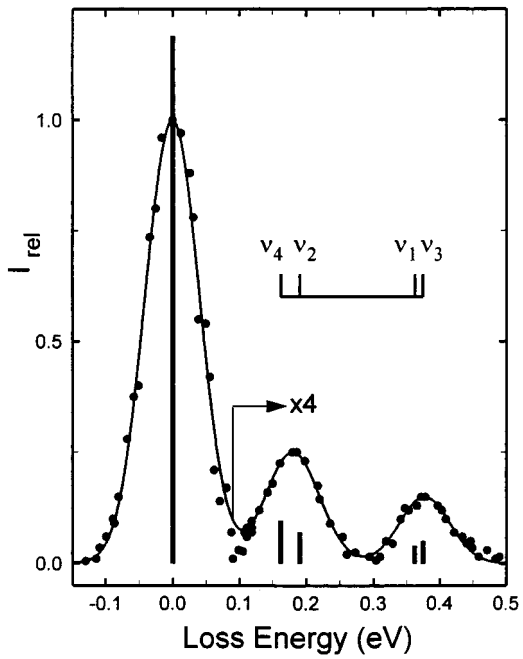

Figure 10. Gas-phase vibrational EELS spectrum[28] of methane at 20 eV and the scattering angle of 120.3°, and the results of 11 × 11 × 11 CGGBS calculations with the inclusion of second-order polarization. The bars represent the calculated differential cross sections. To make them compatible with the spectrum, the differential cross sections for vibrational excitations were multiplied by 4, and then all were scaled with respect to the absolute value[28] ($d\sigma/d\Omega = 0.37$ Å^2/sr) of the differential cross section for elastic scattering. The bars are located at the positions of energies of vibrational fundamentals. The observed (calculated) $\nu_2 + \nu_4$ and $\nu_1 + \nu_3$ cross sections are 2.17 ± 0.23 (1.650) and 1.33 ± 0.15 (0.933) 10^{-18} cm^2/sr, respectively.

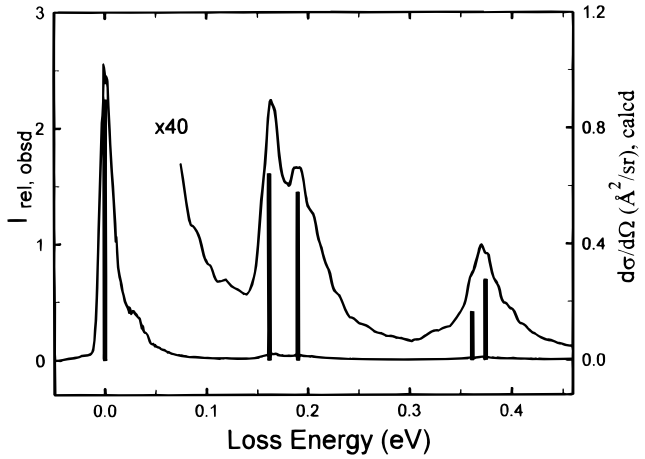

Figure 11. Vibrational EELS of neat solid methane at 20 eV and the scattering angle of 60°. The heights of bars correspond to relative 11 × 11 × 11 CGGBS + polarization intensities. The calculated differential cross sections for vibrational excitation are multiplied by 40 to match the spectrum. The bars are located at the positions of energies of vibrational fundamentals.

As already noted in the Introduction, we are interested primarily in vibrational EELS of polyatomic molecules, and we therefore paid most attention to the methane molecule. For comparison of results of our calculations with experimental results, we selected the paper by Curry et al.[28] To our knowledge, it is the latest paper on vibrational inelastic electron scattering by gaseous CH_4; it seems to give the most complete data, and it also summarizes previous work. Their vibrational EELS spectrum is plotted in Figure 10 together with our calculated differential cross reactions obtained with the 11 × 11 × 11 CGGBS basis set and with the inclusion of second-order polarization. The effect of polarization is small in this case, and also the effect of the size of the CGGBS basis set is small, so qualitatively the same spectral pattern is obtained with 7 × 7 × 7 and 9 × 9 × 9 basis sets and without the polarization. Figure 11 is basically the same as Figure 10, but instead of the gas-phase spectrum of Curry et al.,[28] we present in it the EELS spectrum of solid methane measured at Boulder. The two bending modes are partially resolved in this spectrum, and their relative intensities are reproduced by the calculations. The two stretching modes remain unresolved. Our calculations suggest that the t_2 mode contributes more to the observed intensity than the a_1 mode. The results of our calculations for the electron energy of 20 eV are summarized in Tables 7 and 8. The differential cross sections observed[28] at 20 eV depend very little on the scattering angle. Our calculations are not accurate enough to reproduce this subtle effect, but as Figure 12 shows, they reproduce qualitatively the dependence on the scattering angle for the ratio of intensities of the $\nu_{2,4}$ and $\nu_{1,3}$ bands. We have also calculated differential cross sections for vibrational excitation for electron energies of 7.5, 10, and 15 eV for which experimental data are available.[28] At lower energies, our calculations underestimate the observed increased intensity of vibrational bands, and also the calculated relative intensities seem to be less reliable. However, we think it is premature to analyze these data in more detail when the role of resonance enhancement in the vibrational excitation of CH_4 has not yet been assessed and the experimental data from different laboratories exhibit appreciable scatter.

At the suggestion of a referee we recalculated the vibrational spectrum of methane in the Born approximation. Comparison with the full CGGBS calculation is presented in Table 7. The difference between the two calculated spectra is smaller than we expected, but it is appreciable for some modes and scattering

TABLE 7: Differential Cross Sections of Vibrational Excitation in CH_4 Calculated without the Second-Order Polarization Term[a]

	$d\sigma/d\Omega$ (10^{-18} cm^2/sr)			
scattering angle θ (deg)	ν_4	ν_2	ν_1	ν_3
0	1.011 (0.039)	1.877 (0.051)	1.027 (0.398)	0.397 (0.026)
20	1.304 (1.412)	1.555 (0.223)	0.566 (0.100)	0.390 (0.057)
40	1.438 (2.873)	1.419 (1.431)	0.120 (0.134)	0.491 (0.350)
60	1.407 (2.585)	1.239 (1.865)	0.171 (0.556)	0.539 (0.540)
80	1.369 (2.066)	1.072 (1.637)	0.249 (0.522)	0.637 (0.942)
100	1.106 (1.894)	0.814 (1.408)	0.221 (0.246)	0.627 (1.440)
120	0.935 (1.932)	0.654 (1.162)	0.149 (0.096)	0.449 (1.636)
140	1.207 (2.055)	0.779 (0.995)	0.147 (0.090)	0.627 (1.668)
160	1.857 (2.164)	1.147 (0.940)	0.247 (0.133)	1.306 (1.667)
180	2.223 (2.205)	1.363 (0.934)	0.314 (0.156)	1.722 (1.665)

[a] Electron impact energy: 20 eV; 11 × 11 × 11 CGGBS, no target molecule polarization; the entries in parentheses were obtained in the Born approximation.

TABLE 8: Differential Cross Sections of Vibrational Excitation in CH_4 Calculated with the Second-Order Polarization Term[a]

	$d\sigma/d\Omega$ (10^{-18} cm^2/sr)			
scattering angle θ (deg)	ν_4	ν_2	ν_1	ν_3
0	0.829	2.513	1.937	0.949
20	1.295	2.061	1.061	0.863
40	1.567	1.760	0.287	0.796
60	1.607	1.447	0.414	0.692
80	1.614	1.237	0.602	0.715
100	1.248	0.975	0.607	0.692
120	0.939	0.711	0.392	0.541
140	1.121	0.723	0.284	0.652
160	1.736	1.104	0.454	1.443
180	2.101	1.362	0.594	2.017

[a] Electron impact energy: 20 eV; 11 × 11 × 11 CGGBS.

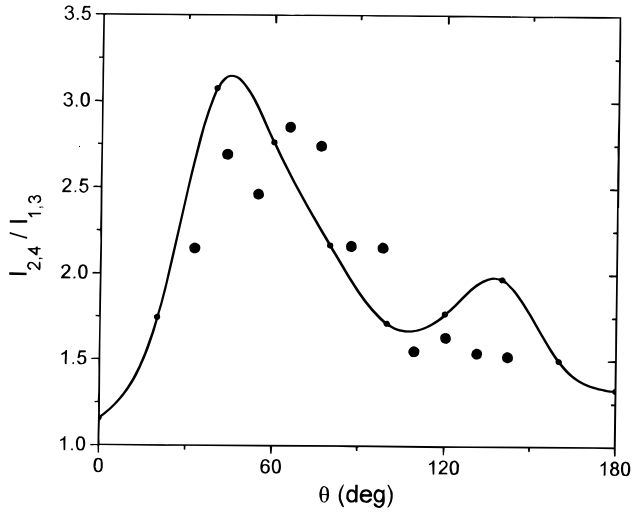

Figure 12. Dependence of the relative differential cross section for vibrational excitations of methane at 20 eV on the scattering angle. $I_{2,4}$ is the sum of vibrational intensities of bending modes ν_2 and ν_4, and $I_{1,3}$ is the sum of vibrational intensities of stretching modes ν_1 and ν_3. The line represents the data calculated with the 11 × 11 × 11 CGGBS with second-order polarization, and the full dots are the relative observed intensities.[28]

angles. The results of the full CGGBS calculation seem to be superior when compared with the observed[28] absolute inelastic cross sections. Still, the Born approximation may be useful in applications to larger molecules and we plan to examine this in more detail.

Conclusions

The results of CGGBS calculations on H_2, H_2O, and CH_4 give a good account of observed elastic and vibrational inelastic electron scattering by these molecules. Of course, in some cases our calculations give results that are inferior to literature data obtained by more sophisticated computational procedures. We emphasize, however, that we are primarily interested in applications to polyatomic molecules, and for these the use of such highly complex procedures would be difficult.

Our present computational scheme is based on a single-channel static-exchange approach with a second-order correction for polarization effects. It is therefore not applicable to low incident electron energies (below about 6 eV), to electronic excitations, and to energies close to resonances. For future practical applications, our present computational method clearly must be extended to a multichannel formulation. Experimentalists measure vibrational inelastic scattering almost exclusively at energies that correspond to resonances,[2] and the progress made in measuring electronic EELS at Boulder[35] also requires progress in calculations.

As our results for methane show, the CGGBS method in its present state may be useful for predicting the pattern of vibrational EELS spectra of nonpolar polyatomic molecules for electron energies of about 20 eV, above the critical region of resonances. We have already started calculations on acetylene, ethylene, and ethane, which belong to a set of small molecules selected for matrix-isolation EELS experiments at Boulder.

Acknowledgment. This work was supported by the U.S.−Czechoslovak Science and Technology Program (Grant 93018), the Grant Agency of the Czech Republic (Grant 203/96/1072), NATO (Grant 951530), and the NSF (Grants CHE-9318469 and CHE-9412767).

References and Notes

(1) Allan, M. *J. Electron Spectrosc. Relat. Phenom.* **1989**, *48*, 219.
(2) Allan, M. *Chimia* **1994**, *48*, 372.
(3) Kuppermann, A.; Flicker, W. M.; Mosher, O. A. *Chem. Rev.* **1979**, *79*, 77.
(4) Jordan, K. D.; Burrow, P. D. *Chem. Rev.* **1978**, *87*, 557.
(5) Lucchese, R. R.; Takatsuka, K.; McKoy, V. *Phys. Rep.* **1986**, *131*, 147.
(6) Winstead, C.; McKoy, V. *Modern Electronic Structure Theory*; Yarkony, D. R., Ed.; World Scientific: Singapore, 1995.
(7) Čársky, P.; Hrouda, V.; Michl, J. *Int. J. Quantum Chem.* **1995**, *53*, 419.
(8) Čársky, P.; Hrouda, V.; Michl, J. *Int. J. Quantum Chem.* **1995**, *53*, 431.
(9) Čársky, P.; Hrouda, V.; Michl, J.; Antic, D. *Int. J. Quantum Chem.* **1995**, *53*, 437.
(10) Hrouda, V.; Polášek, M.; Čársky, P.; Michl, J. *Theor. Chim. Acta* **1994**, *89*, 401.
(11) Polášek, M.; Čársky, P. *Czech. J. Phys.* **1995**, *45*, 735.
(12) Rescigno, T. N.; McCurdy, C. W.; McKoy, V. *Chem. Phys. Lett.* **1974**, *27*, 401.
(13) Klonover, A.; Kaldor, U. *Chem. Phys. Lett.* **1977**, *51*, 321.
(14) Lane, N. F. *Rev. Mod. Phys.* **1980,** *52*, 29.
(15) Gianturco, F. A.; Jain, A. *Phys. Rep.* **1986**, *143*, 347.
(16) Sun, Q.; Winstead, C.; McKoy, V.; Lima, M. A. P. *J. Chem. Phys.* **1992**, *96*, 3531.
(17) Winstead, C.; Sun, Q.; McKoy, V. *J. Chem. Phys.* **1992**, *96*, 4246.
(18) Winstead, C.; Sun, Q.; McKoy, V. *J. Chem. Phys.* **1992**, *97*, 9483.
(19) Sadlej, A. J. *Collect. Czech. Chem. Commun.* **1988**, *53*, 1995.
(20) Pople, J. A.; Krishnan, R.; Schlegel, H. B.; Binkley, J. S. *Int. J. Quantum Chem. Symp.* **1979**, *13*, 225.
(21) Srivastava, S. K.; Chutjian, A.; Trajmar, S. *J. Chem. Phys.* **1975**, *63*, 2659.
(22) Trajmar, S.; Register, D. F.; Chutjian, A. *Phys. Rep.* **1983**, *97*, 221.
(23) Nishimura, H.; Danjo, A.; Sugahara, H. *J. Phys. Soc. Jpn.* **1985**, *54*, 1757.
(24) Huzinaga, S. *J. Chem. Phys.* **1965**, *42*, 1293.
(25) Lima, M. A. P.; Gibson, T. L.; Huo, W. M.; KcKoy, V. *Phys. Rev. A.* **1985**, *32*, 2696.
(26) Shyn, T. W.; Cho, S. Y. *Phys. Rev. A* **1987**, *36*, 5138.
(27) Johnstone, W. M.; Newell, W. R. *J. Phys. B* **1991**, *24*, 3633.
(28) Curry, P. J.; Newell, W. R.; Smith, A. C. H. *J. Phys. B* **1985**, *18*, 2303.
(29) Tanaka, H.; Okada, T.; Boesten, L.; Suzuki, T.; Yamamoto, T.; Kubo, M. *J. Phys. B* **1982**, *15*, 3305.
(30) Boesten, L.; Tanaka, H. *J. Phys. B* **1991**, *24*, 821.
(31) Lima, M. A. P.; Watari, K.; McKoy, V. *Phys. Rev. A* **1989**, *39*, 4312.
(32) Linder, F.; Schmidt, H. *Z. Naturforsch.* **1971**, *26A*, 1603.
(33) Seng, G.; Linder, F. *J. Phys. B* **1976**, *9*, 2539.
(34) Shyn, T. W.; Cho, S. Y.; Cravens, T. E. *Phys. Rev. A* **1988**, *38*, 678.
(35) Antic, D.; David, D. E.; Michl, J. 15th IUPAC Symposium on Photochemistry, Prague, Czech Republic, 1994; Abstract 260.